Oil & Natural Gas Technology

DOE Award No.: DE-FE0009904

Quarterly Research Performance Progress Report (Period ending 12/31/2014)

Structural and Stratigraphic Controls on Methane Hydrate occurrence and distribution: Gulf of Mexico, Walker Ridge 313 and Green Canyon 955

Project Period: 10/01/2012 – 09/30/2015

Submitted by:

Priyank Jaiswal

Signature

Office of Fossil Energy

Executive Summary

This quarterly progress summarizes the progress made towards completion of Phase 2, Subtask 3.2 – 3.4 which comprises Full Waveform Inversion (FWI) of OBS data acquired by the USGS in the leased block Walker Ridge 313.

Background

The overall objective is to identify and understand structural and stratigraphic controls on hydrate accumulation and distribution in leased blocks WR313 (WR: Walker Ridge) and GC955 (GC: Green Canyon) in the Gulf of Mexico using seismic and well data (Figure 1). The effort is to be completed in three phases. In the first phase, the objective is to create a large-sale (resolution in the order of Fresnel zone) P-wave velocity model using traveltime inversion and a corresponding depth image using pre-stack depth migration (PSDM). This phase was completed in due time.

In the second phase, which is the topic of this report, the objective is to refine the resolution of the P-wave velocity model created in the first phase to the order of seismic wavelength using full-waveform inversion and simultaneously create P-wave velocity (V_P) and P-wave attenuation (Q_P^{-1}) model. At this stage, we have completed the second phase on both the GC and WR datasets. In the Q3 report the updated velocity and attenuation model for the GC dataset were presented. In this report the updated velocity model for the WR313 datasets are being presented.

The third phase has two objectives. The first objective is to create a hydrate distribution map with the help of P-wave velocity and attenuation model created in the second phase and standard rock physics modeling method. The second objective is to jointly interpret the saturation map, Full-Waveform Inversion (FWI) velocity and attenuation, and the PSDM image to determine the structural and stratigraphic controls on hydrate occurrence and distribution.

Approach

Previously both OBS and MCS data, obtained from USGS, we set up for processing in ProMAX© processing software using the navigation data made available from the field (Figure 1). After setting up the navigation, the data were imported into and visually verified for their correctness. Following this, the OBS data were processed for clock drift and processed. The MCS data were also processed to create a stack. The stacked data were then depth migrated and verified with the well depths. A large-sale (resolution in the order of Fresnel zone) P-wave velocity model using traveltime inversion and a corresponding depth image using pre-stack depth migration (PSDM) were generated through inversion using an approach known as Unified Imaging (UI), which was developed by Jaiswal and Zelt (2008) as a way of testing the Deragowski principle, i.e, the consistency of a velocity model with its corresponding depth migrated image. The velocity profile from traveltime inversion generally captures the background trends but it is not show the details to explain the distribution of gas hydrate and free gas. This model is refined using Full Waveform Inversion (FWI).

We applied frequency-domain full waveform inversion (FWI) (Pratt, 1999) to the 9 OBS data (Fig. 1) in order to obtain a quantitative, high-resolution P-wave velocity model and the attenuation model. In this approach, the required forward simulations use a frequency-domain finite difference method. FWI employs local gradient method for model optimization, in which the gradients are calculated using a back-propagation of misfits of the real wavefield and the modelling wavefield. Since FWI is a strongly non-linear inverse problem, the traveltime inversion model was used as an initial model. In order to use an FWI with the real data, a series of data preprocessing steps were required including deconvolution, resampling and windowing. The near offset (up to ±0.5 km) were also eliminated due to the observed amplitude saturation of early arrivals. Wavenumber filtering was applied to each successive gradient image, in order to mitigate receiver-side spatial aliasing, and also to enhance the recovery of low spatial wavernumber of the images at the early stages of the inversion process. The source wavelet was repeatedly re-estimated from data after each velocity update step using the linear optimization method (Pratt, 1999). Attenuation in the Pratt (1999) method is mainly a result of absorption. Attenuation is included in the inversion by specifying the velocity model (m) as a complex quantity ($m = m_r + im_i$), where the imaginary (m_i) and real (m_r) parts are related through the seismic quality factor Q (the reciprocal of attenuation) as

$$m_i = -\frac{m_r}{2Q}.$$

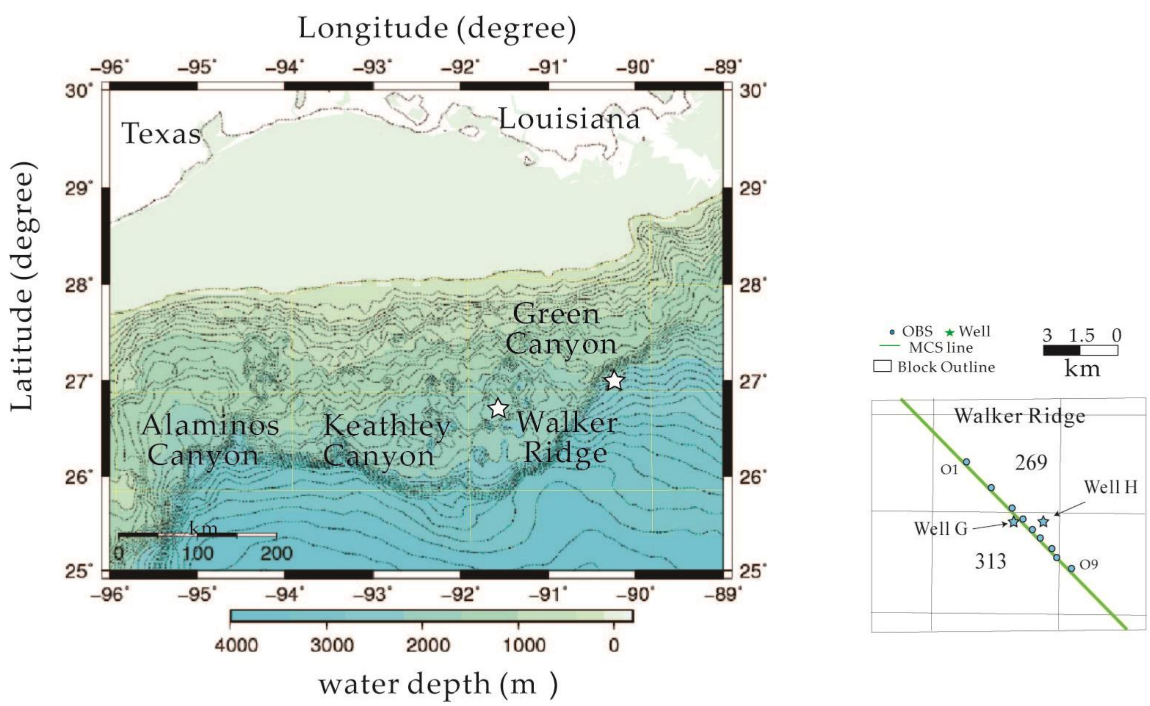

Figure 1. Base map. Seafloor bathymetry of Gulf of Mexico showing the location of the study area at the mouth of Green Canyon. The acquisition layout within the leased block 313 (WR313) is shown in the inset. Solid line is the track of the Multi-Channel Seismic (MCS) profile. Solid circles are location of Ocean Bottom Seismometers (OBSs) O1 – O9. Solid stars mark the locations of the wells G and H that were drilling during the Joint Industry Project Leg II (JIP II).

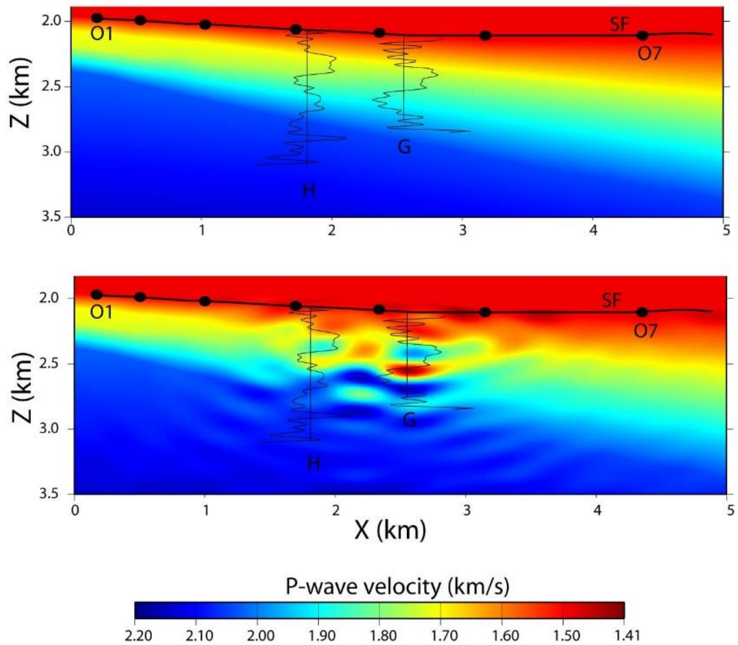

Figure 2. P-wave velocity (V_P) models. (a) Starting model from composite traveltime inversion – depth migration (b) Final model from FWI. Symbols have the following meanings. SF is the seafloor; O1 – 7 are OBS locations; and G and H are the well locations. Sonic logs are overlaid along the respective wells.

The initial model for FWI was the final V_P model developed from traveltime inversion (Figure 2a). Only a partial region (distance 2.0 – 7.0 km) of original model which was 11.0 wide is used for FWI due to calculation efficiency. The initial source for FWI was a minimum phase ricker wavelet. As a first step, using the traveltime model, a new source was estimated. Based on the reciprocity principle, OBSs were assumed as sources and the ship locations from where the actual shots were fired were assumed as receivers. Thus, the source inversion required only seven independent source corresponding to seven OBS gathers. The first inverted source was used for forward modeling to ensure the simulated seafloor arrivals are within half-cycle of the field seafloor arrivals. Next, keeping this source and the traveltime model stationary, the minimum frequencies in the data, 7.25, 7.5 and 7.75 Hz were simultaneously inverted resulting in very broad and smooth updates (Figure 3a). Next, with the inverted V_P model, a new source was estimated and the process was repeated for groups of frequencies up to 14.75 Hz. Each group comprised 3 frequencies space 0.25Hz apart.

Essential to obtaining meaningful result from FWI was cosine tapering of the gradient at the seafloor to balance the updates in the deeper subsurface. The iterative inversion in each frequency group was halted after the reduction in the misfit function was less than 1%. The V_P model became excessively noisy after the inversion of 14.75 Hz. FWI was halted at this stage. Between the minimum and maximum frequencies, inversion of only two frequency groups, 9.25 – 9.75 Hz (Figure 3b) and 12.25 – 12.75 Hz (Figure 3f), resulted in reasonably large updates (5% or higher) in their respective models.

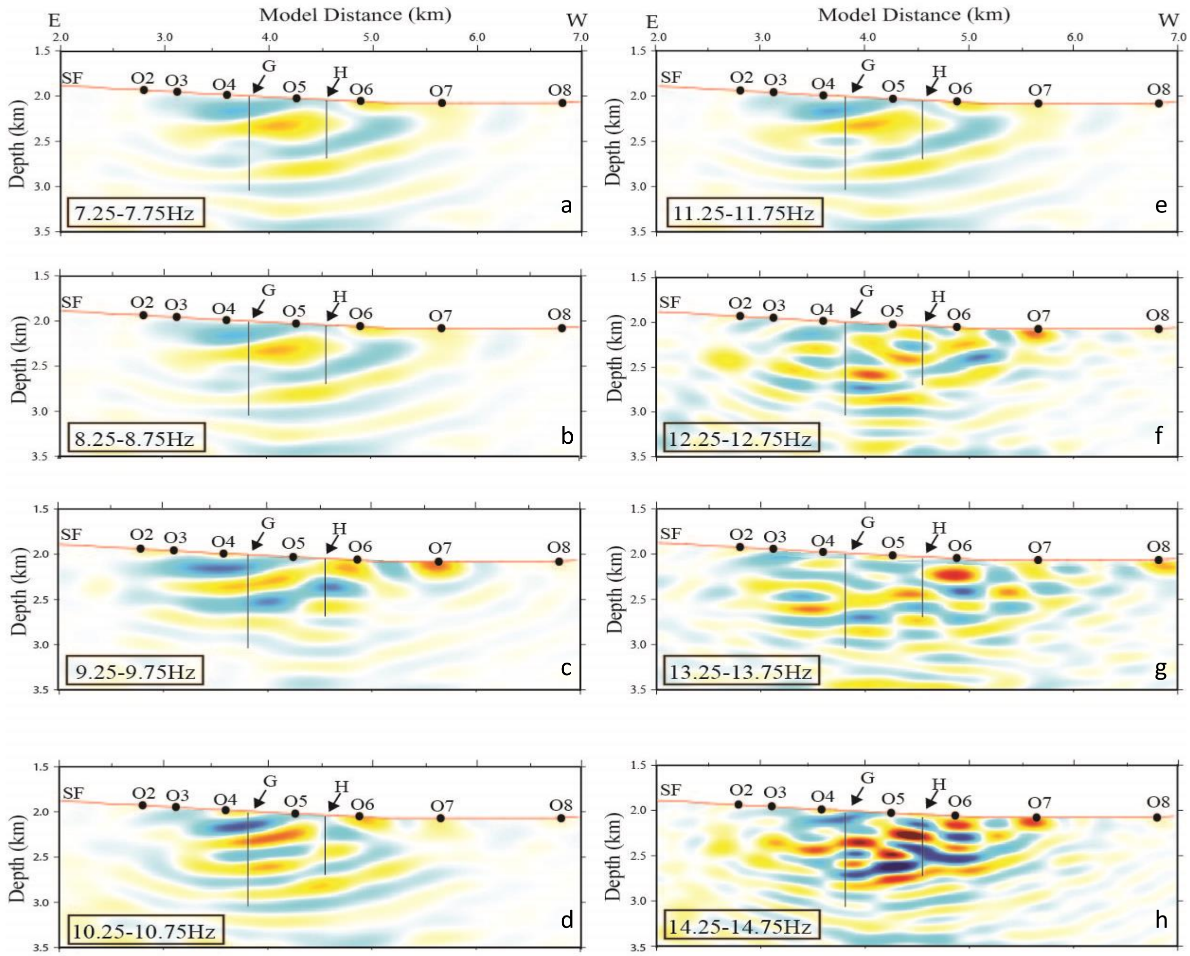

Figure 3. Velocity perturbations between the initial model and updated model. Model in (a) through (e) are from inversion of 2.25-2.75 Hz, 6.25-6.75 Hz, 9.25-9.75 Hz, 13.25-13.75 Hz, 17.25-17.75 Hz. The curves at the wells show the velocity perturbations between the initial model and the log velocity.

Results:

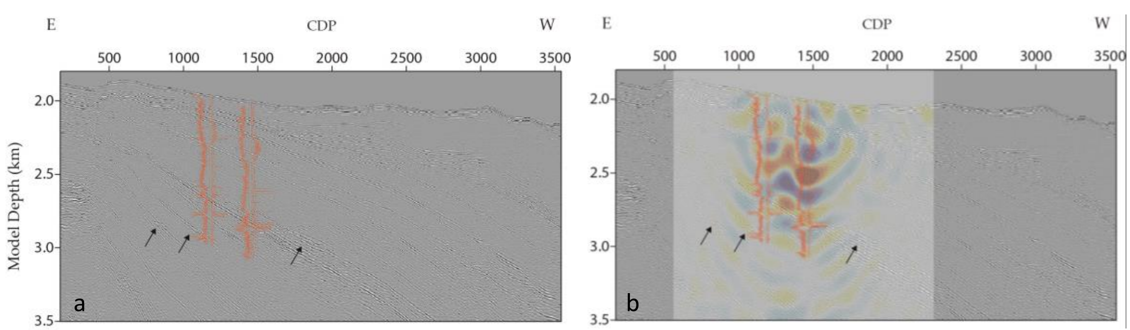

Figure 4. Composite interpretation. (a) Final depth image. (b) Overlay of the final depth image and final VP perturbations. In (a) and (b) black arrows indicate hydrate-rich horizons. The left and the right tracks along the wellbore are sonic and resistivity respectively.

Although the depth image appears to be realistic and corresponds with the wells G and H (Figure 4a), an overlay of the depth image and the final perturbation model does not show good correspondence (Figure 4b). The perturbations are more scattered above the hydrate bearing horizons than what is expected, which probably indicates compartmentalized but with no bearings on the internal connectivity. It is possible that these perturbations are somewhat unrealistic and data artefacts.

In absence of the sonic logs, it is impossible to relate the V_P perturbations to hydrate or free gas. The sonic logs in wells G and H suggested over 20% V_P increase over the background within the hydrate-bearing sands. The seismic, however, showed only a modest increase of ~10%. It does not imply that sonic frequencies were insensitive to hydrates, but that they see an averaged effect over a larger volume of sediments than the logs. The velocity anomaly is seismic could have matched the well logs probably if the hydrate-bearing sands were spatially (both vertically and laterally) more extensive. Within the stratigraphy, the maximum velocity increase is at the location of Well H (Figure 4b) in the hydrate-bearing clay horizons. This is somewhat counter-intuitive and therefore the inversion for WR313 needs to be reconsidered. Away from the wells G and H, within the resolution of seismic only a modest presence of hydrate or free gas can be speculated. Away from the wells, the positive and negative perturbations could also be indicative of lithological changes rather than hydrate and free gas variation.

Conclusions:

FWI yielded reliable estimates even with a visco-acoustic approximation to an elastic dataset. Success of FWI strongly depends on data preconditioning and the starting model. The minimum and the maximum usable inversion frequencies were 7.25 and 14.75 Hz respectively. In between, frequencies spaced 0.25Hz apart were inverted in groups of 3. A multi-scale FWI approach prevents cycle-skipping. A composite reflectivity and V_P interpretation suggests that both hydrate and free gas have a patchy distribution.

References:

Jaiswal, P., and C. A. Zelt. 2008, Unified imaging of multichannel seismic data: Combining traveltime inversion and prestack depth migration. Geophysics, 73, no. 5, VE269-VE280. doi: 10.1190/1.2957761.

Jaiswal P., P. Dewangan, T. Ramprasad, C.A. Zelt, 2012. Seismic characterization of hydrates in faulted, fine-grained sediments of Krishna-Godavari Basin: Full Waveform Inversion: Journal of Geophysical Research – Solid Earth, 117, B10305.Pratt, R.G., 1999. Seismic waveform inversion in the frequency domain, Part 1: Theory, and verification in a physical scale model. Geophysics, 64, 888-901.

White, J. 1975, Computed seismic speeds and attenuation in rocks with partial gas saturation. Geophysics, 40, no. 2,224-232. doi: doi:10.1190/1.1440520.

Project milestone chart

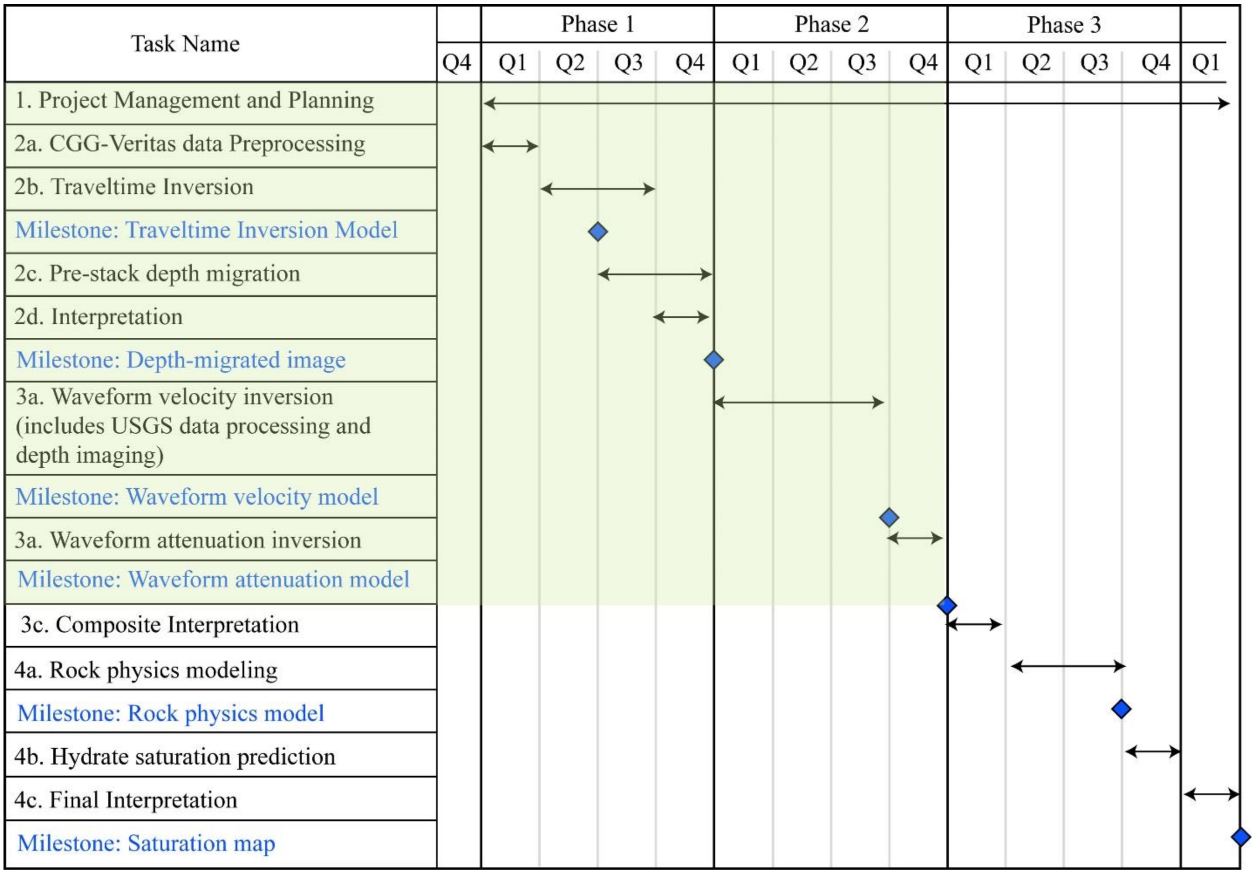

The project is on target till date. Tasks already completed in the milestone chart are shaded in green.

Milestone Status:

Milestone	Description	Status	Schedule
Traveltime Inversion Model	The recipient shall compare the real and predicted reflection traveltimes from the final velocity model to be used for PSDM.	Done for CGGVeritas Datase and for the USGS dataset	Completed on target
Depth Migrated Image	The recipient shall compare structure and stratigraphy between the final depth image and images in literature and SSRs.	Done	Completed on target
Waveform velocity model	The recipient shall compare waveform inversion velocity and sonic logs at well locations.	Done	Completed On target
Waveform attenuation model	The recipient shall compare real and synthetic simulated data.	Done	Completed On target
Rock physics model	The recipient shall compare predicted hydrate saturation at well locations with that available in the literature and methods of other DOE funded PIs, if available.	Ongoing	On target
Saturation map	The recipient shall compare consistency between hydrate distribution and structural/stratigraphic features interpreted in the study area.	Ongoing	On target

National Energy Technology Laboratory

626 Cochrans Mill Road

P.O. Box 10940

Pittsburgh, PA 15236-0940

3610 Collins Ferry Road

P.O. Box 880

Morgantown, WV 26507-0880

13131 Dairy Ashford Road, Suite 225

Sugar Land, TX 77478

1450 Queen Avenue SW
Albany, OR 97321-2198

Arctic Energy Office

420 L Street, Suite 305

Anchorage, AK 99501

Visit the NETL website at:

www.netl.doe.gov

Customer Service Line: 1-800-553-7681